

A CONCURRENTLY COUPLED MULTI-SCALE MODEL FOR PREDICTING PROPERTIES OF THERMOPLASTIC AND THERMOSET NANOCOMPOSITES

Samit Roy^{1*}, Avinash Reddy Akepati¹, Nicholas hayes¹

¹ Dept. of Aerospace Engineering and Mechanics, University of Alabama, Tuscaloosa, AL 35487
*sroy@eng.ua.edu

Keywords: Molecular dynamics, J-integral, multi-scale modeling, nano-particle reinforced polymers.

Abstract

Over the past decade, mechanical characterization data for nanoparticle reinforced polymer matrix composites (PMC) has shown significant improvements in compressive strength and interlaminar shear strength in comparison with baseline properties. While the synergistic reinforcing influence of nanoparticle reinforcement is obvious, a simple rule-of-mixtures approach fails to quantify the dramatic increase in mechanical properties. Consequently, there is an immediate need to investigate and understand the mechanisms at the nanoscale that are responsible for such unprecedented strength enhancements. A multi-scale and multi-physics simulation approach is considered computationally more viable since relying on a single time or length scale may require huge amounts of computational resources and can potentially lead to inaccurate results. A proof-of-concept case study involving crack initiation in a graphene nano-platelet is presented, together with a methodology for computing the atomistic J-integral based on Hardy estimates of continuum fields. The same methodology will be used to gain a better understanding of the influence of nanoscale phenomena on continuum scale mechanical properties of a polymer nanocomposite. It is envisioned that the current research will contribute towards the understanding of advanced nanostructured composite materials within the context of Integrated Computational Materials Engineering (ICME).

1 Introduction

Figure 1 shows the length scales involved in a typical nanoparticle reinforced fiber-reinforced polymer-matrix composite. The nanoparticle reinforcements are nanometer ($\sim 10^{-9}$ meters) thick particles that interact intimately with the polymer matrix molecules to provide strengthening of the polymer matrix at the nano-scale. The size of the polymer molecules are roughly on the order of the nanoparticle thickness, depending on the degree of polymerization. Moving up the scale we find that the carbon fiber diameter is usually on the order of 5 to 10 microns, although its length may extend up to several meters. The composite (matrix reinforced with fiber) is in the macro or engineering-scale of analysis. The combination of fiber reinforcements in the polymer matrix gives the macro-scale composite

orthotropic properties. The nano-scale interaction between polymer molecules and nanoparticle is a key factor in determining the macro-scale strength of the composite.

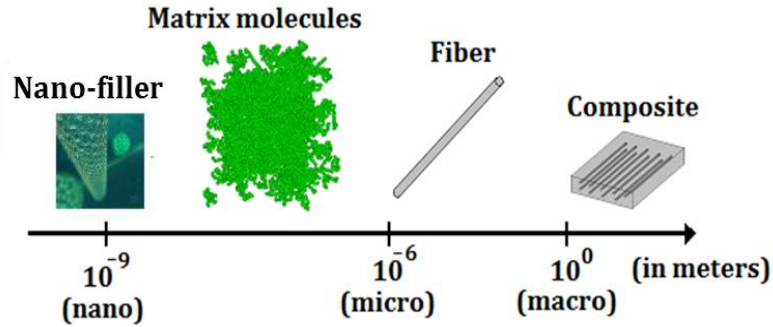


Figure 1. Length scales involved in multi-scale modeling

In recent years numerous efforts have been directed towards modeling nanocomposites in order to better understand the reasons behind the enhancement of mechanical properties, even by the slight addition (a few weight percent) of nano-materials [1-12]. In studying molecular systems however, a multi-scale and multi-physics simulation approach is considered computationally more viable since relying on a single time or length scale can take a huge amount of computational resources and can potentially lead to inaccurate results.

2 Molecular Dynamics

Because it is now well-established that the complex interactions at molecular level can only be understood by numerical methods which appeal to theoretical formalisms at the nano-scale, we look to use molecular dynamics (MD) to analyze and understand small-scale phenomena. The ability to simulate large number of atoms (atomic systems simulated by MD are typically much larger ab-initio methods, see Khare et al [11]) allows us to have better statistical estimates of system thermodynamic properties such as thermal conductivity and mechanical properties such as the Young's modulus. By retaining the level of detail required to describe the structure of atomic systems coupled with the selection of proper force-field parameters to accurately describe the various molecular interactions (see e.g. Allen and Tildesley [13]) we can closely simulate the necessary bulk properties of any system.

For a N atom, molecular system we have the equation motion of atom 'i' as,

$$m_i \ddot{\mathbf{x}}_i^t = - \frac{\partial V(\mathbf{x}_1^t, \mathbf{x}_2^t, \dots, \mathbf{x}_N^t)}{\partial \mathbf{x}_i^t} \equiv \mathbf{F}_i^t \quad (i = 1, 2, \dots, N) \quad (1)$$

In molecular dynamics the atomistic structure at initial time (\mathbf{r}_i^0) is input to the algorithm, with the required force fields chosen to describe the various atomic interactions. The internal force at any atom i , \mathbf{F}_i is computed from the energy potential (V) chosen by the user (see Eq. (1)).

3 Background on Multi-scale Modeling

There are two unique choices in multi-scale modeling, namely, the hierarchical and concurrent simulations scheme. In the hierarchical approach the physical system is studied in isolation to far-field stimuli and the results are translated to a continuum response using curve fits and/or statistical averaging. Valavala et al [3] used the energy equivalence of continuum and atomistic models of polymer systems to characterize the nonlinear stress-strain response

of polymers (in particular, polycarbonate and polyimide). Burchyachenko et al [4] used the Eshelby and Mori-Tanaka methods to determine the effective properties of nanocomposite materials. Riddick et al [5] used equivalent modeling of carbon nanotubes in polymers to study the fracture toughness of polymer matrix composites with carbon nanotubes (CNTs) embedded in them. Awasthi et al [6] employed molecular dynamics (MD) to determine the force-displacement curves between nano-inclusions (CNT) and the polymer system. A detailed discussion on multi-scale modeling has been presented by Roy et al [14].

Although there have been many attempts to model standard solid lattice structures and couple them to various continuum methods, to our knowledge, large scale concurrent coupling of nanoparticle reinforced polymer systems has not been attempted before. One of the reasons why a polymer system coupling has never been attempted before is because of the complexity involved in modeling polymers. Under ambient conditions the polymer model is amorphous (depending on the degree of crystallinity) and lacks specific ordered structure. Further, a polymer MD model takes longer time to equilibrate as compared with an ordered lattice. We envision that the work in this paper will contribute towards the fundamental understanding of nanoscale interactions in nanostructured composite materials, as described in the next section.

4 Atomistic J-integral Evaluation Methodology

Our goal is to be able to use MD simulations to compute a nanomaterials performance metric, such as the atomistic J-Integral, in order to quantify the influence of nano-fillers such as graphene platelets on phenomenon such as delamination crack propagation in a laminated composite, as depicted in Figure 2. The J-integral evaluation scheme discussed below can be subsequently applied to polymeric systems to evaluate fracture metrics, such as work of separation. These data can then be employed in a multi-scale model using concurrent coupling discussed earlier. In this paper, the feasibility of computing the J-integral over a purely MD domain at finite temperatures using Hardy estimates of continuum fields for a polymer system is evaluated. In conventional macro-scale fracture mechanics, the J-integral vector, defined as the divergence of the Eshelby stress tensor (refer to Eqn. (2)), has been used to quantify the crack driving force available from thermo-mechanical loading as well as material inhomogeneities.

$$\mathbf{J} = \int_{\partial\Omega} \underline{S} \underline{N} dA = \int_{\partial\Omega} (\Psi \underline{N} - \underline{F}^T \underline{P} \underline{N}) dA \quad (2)$$

In Eqn. (2), \underline{S} is the Eshelby stress tensor, Ψ is the free energy density, \underline{F} is the deformation gradient tensor, \underline{P} is the first Piola-Kirchhoff stress tensor, \underline{N} is the outward normal to the surface $\partial\Omega$ along which contour the J-integral is being evaluated. At a temperature of 0 K and equilibrium, Eqn. (2) reduces to Eqn. (3), where W is the stored energy density and \underline{H} is the displacement gradient.

$$\mathbf{J} = \int_{\partial\Omega} (W \underline{N} - \underline{H}^T \underline{P} \underline{N}) dA \quad (3)$$

The critical value of J_I at crack initiation is related to the fracture toughness of the material, where the subscript I denotes the fracture mode (I=1,2,3). Therefore, the J-integral could be used as a suitable metric for estimating the crack driving force as well as the fracture toughness of the material as the crack begins to initiate. However, for the conventional macroscale definition of the J-integral to be valid at the nanoscale in terms of the continuum stress and displacement fields (and their spatial derivatives) requires the construction of local

continuum fields from discrete atomistic data, and using these data in the conventional contour integral expression for J, as given by Eqn. (2) [15,16].

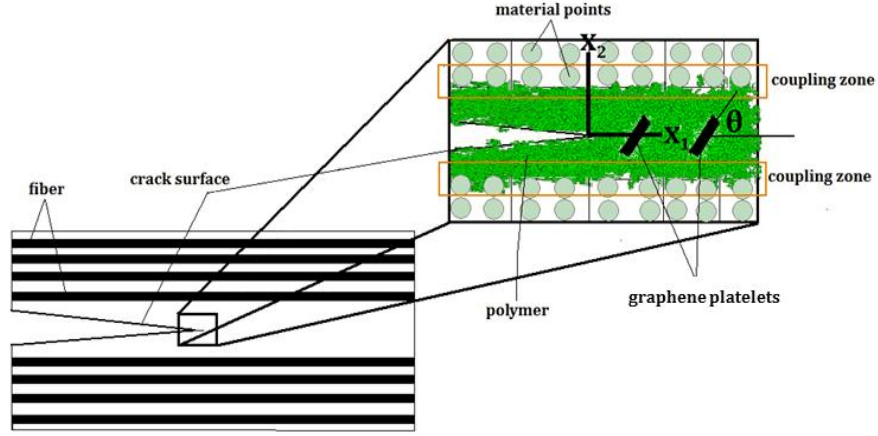


Figure 2. Delamination crack propagation

One such methodology is proposed by Hardy [17] , that allows for the local averaging necessary to obtain the definition of free energy, deformation gradient, and Piola-Kirchoff stress as fields (and divergence of fields) and not just as total system averages. Here it is assumed that ensemble average $\langle \cdot \rangle^*$ is approximated by the time average of the quantity over a sufficiently long period of time. A detailed description for evaluation of each term required to calculate atomistic J-integral is given below.

The stored energy density field (W) can be expressed as a sum of atomistic potentials of each atom using Eqn. (4).

$$W(\mathbf{X}, t) = \sum_{\alpha=1}^M (\phi^\alpha(t) - \phi_x^\alpha) \psi(\mathbf{X} - \mathbf{X}^\alpha) = \sum_{\alpha=1}^M \phi^\alpha(t) \psi(\mathbf{X} - \mathbf{X}^\alpha) - W(\mathbf{X}) \quad (4)$$

In Eqn. (4), ϕ^α is atomistic potential, ϕ_x^α is the reference potential energy density of at 0 K, ψ is the localization function, M is the number of atoms and $W(\mathbf{X})$ is a constant. Dividing the domain into localization boxes, the atomistic potential at the centroid of the box can be defined using Eqn. (5) and the field distribution of the potential over the domain is given by Eqn. (6), where $N_I(\mathbf{X})$ are interpolation functions.

$$\phi_I(\mathbf{X}_I, t) = \sum_{\alpha=1}^M \psi_{I\alpha}(\mathbf{X}^\alpha - \mathbf{X}_I) \phi^\alpha(t) \quad (5)$$

$$\phi(\mathbf{X}, t) = \sum_{I=1}^N N_I(\mathbf{X}) \phi_I(\mathbf{X}_I, t) \quad (6)$$

Substituting Eqn. (6), in Eqn. (4), gives the final expression for calculating the stored energy density field, given by Eqn. (7).

$$W(\mathbf{X}, t) = \sum_{I=1}^N \sum_{\alpha=1}^M N_I(\mathbf{X}) \psi_{I\alpha}(\mathbf{X}^\alpha - \mathbf{X}_I) \phi^\alpha(t) - W(\mathbf{X}) \quad (7)$$

As originally proposed by Hardy [17], the localization function depends on the location of the atom in the localization box. The function has to satisfy the properties of $\psi > 0$ and $\int_{\Omega} \psi dV = 1$.

Referring to Figure 3, localization function used in this paper is given by Eqn. (8).

$$\psi(\mathbf{X} - \mathbf{X}^\alpha) = \begin{cases} X_I - \frac{L_x}{2} \leq X^\alpha \leq X_I + \frac{L_x}{2} \\ \frac{1}{L_x L_y L_z} \text{ if } Y_I - \frac{L_y}{2} \leq Y^\alpha \leq Y_I + \frac{L_y}{2} \\ Z_I - \frac{L_z}{2} \leq Z^\alpha \leq Z_I + \frac{L_z}{2} \\ 0 \end{cases} \quad (8)$$

where, L_x , L_y and L_z are the dimensions of the localization box and X_I , Y_I and Z_I are the coordinates of the centroid, as illustrated in Figure 3. In a similar way, displacement gradient can be evaluated using Eqn. (9), where $\mathbf{u}(\mathbf{X}, t)$ is the displacement vector.

$$\underline{H}(\mathbf{X}, t) = \nabla_x \mathbf{u}(\mathbf{X}, t) = \sum_{I=1}^N \sum_{\alpha=1}^M \nabla_x N_I(\mathbf{X}) \psi_{I\alpha}(\mathbf{X}^\alpha - \mathbf{X}_I) \mathbf{u}^\alpha(t) \quad (9)$$

The so-called ‘‘bond function’’ $B_{\alpha\beta} = \int_0^1 \psi(\lambda(\mathbf{X}_\alpha - \mathbf{X}) + (1-\lambda)(\mathbf{X}_\beta - \mathbf{X})) d\lambda$ as defined by Hardy [17] can then be used to compute the first Piola-Kirchoff stress along the contour as given by Eqn. (10),

$$\underline{P}(\mathbf{X}, t) = -\frac{1}{2} \sum_{\alpha=1}^M \sum_{\beta \neq \alpha}^M \mathbf{f}^{\alpha\beta} \otimes \mathbf{X}^{\alpha\beta} B^{\alpha\beta}(\mathbf{X}) \quad (10)$$

where, $\mathbf{f}^{\alpha\beta}$ is the force between atoms α and β , and $\mathbf{X}^{\alpha\beta}$ is the difference in their positions. The free energy density $\Psi = U - TS = -\frac{k_B T}{V} \text{Log} Z$, where U is the internal energy density, T is the temperature, S is the entropy density, V is the volume of the ensemble and Z is the partition function of the atoms occupying the region Ω .

Note that our general definition of free energy density Ψ includes the entropy term and therefore is valid for finite temperature applications of the atomistic J-integral. In [16], a local harmonic (LH) approximation based on the Cauchy-Born model was used to compute the partition function (Z) for an idealized material with defect free crystalline structure at finite (non-zero) temperature. However, the LH approximation is not valid for an amorphous (disordered) cross-linked polymer network [15].

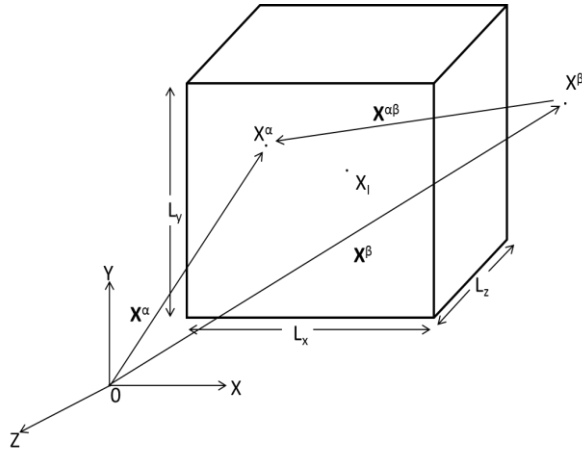


Figure 3. Illustration of a localization box with one atom inside and another outside the box

5 Preliminary Results for Atomistic J-integral Computation

Numerical integration through Gaussian quadrature was employed to evaluate atomistic J-integral using the equations discussed in the previous section (Eqs. (2-10)). Figure 4 shows the Gaussian quadrature points as red dots along the integration contour (solid line). As a preliminary demonstration of the feasibility of atomistic J-integral approach, we simulated mode I (opening mode) nanoscale crack in a single graphene platelet, as depicted in Figure 6(A).

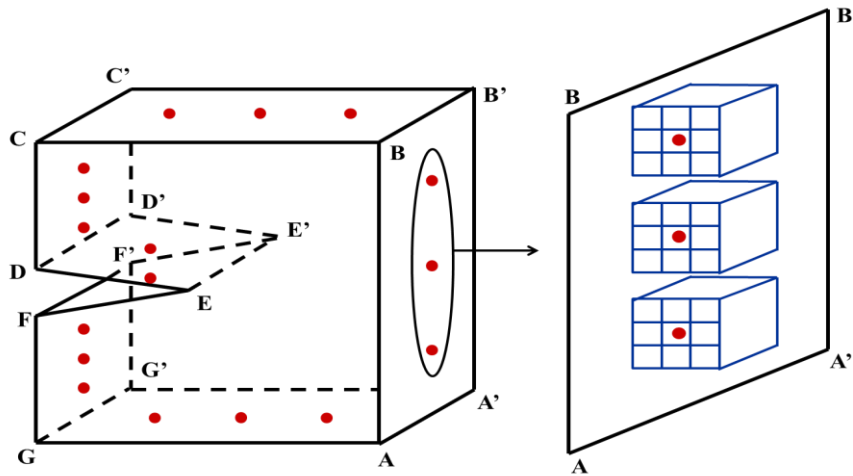


Figure 4. Gaussian quadrature points along the integration contour depicting localization boxes on one side.

In this example the graphene platelet is modeled in LAMMPS using harmonic style for bonds and angles, and OPLS style for dihedrals. The graphene platelet was subjected to a far field uniaxial stress normal to the crack, and the atomistic J-integral was computed on the contour as shown in the Figure 5(A). In order to establish proof-of-concept for atomistic J-integral computation, the MD simulations were carried out isothermally at temperature $T = 0$ K, that is, without any entropic contribution to the free energy. Pressure barostatting was not used in these simulations. The localization box size used for these computations was 0.3 nanometers. The initial length of the pre-existing (starter) crack was set equal to 0.6 nanometers in the

graphene platelet. The coarse time-step for the problem (Δt) was set equal to 0.01 femtoseconds. Figure 5(A) shows the MD simulation of the initiation of a nanoscale dynamic mode I crack in the graphene platelet. The normalized atomistic J-integral results are shown in Figure 5(B) for a graphene platelet and compared with linear elastic fracture mechanics (LEFM) predictions. The figure shows that the quadratic dependence of the normalized atomistic J-integral on mode I stress intensity factor (K_I) is in good agreement with LEFM predictions. Work is currently underway to rigorously benchmark the atomistic J-integral for amorphous polymeric systems at finite temperatures.

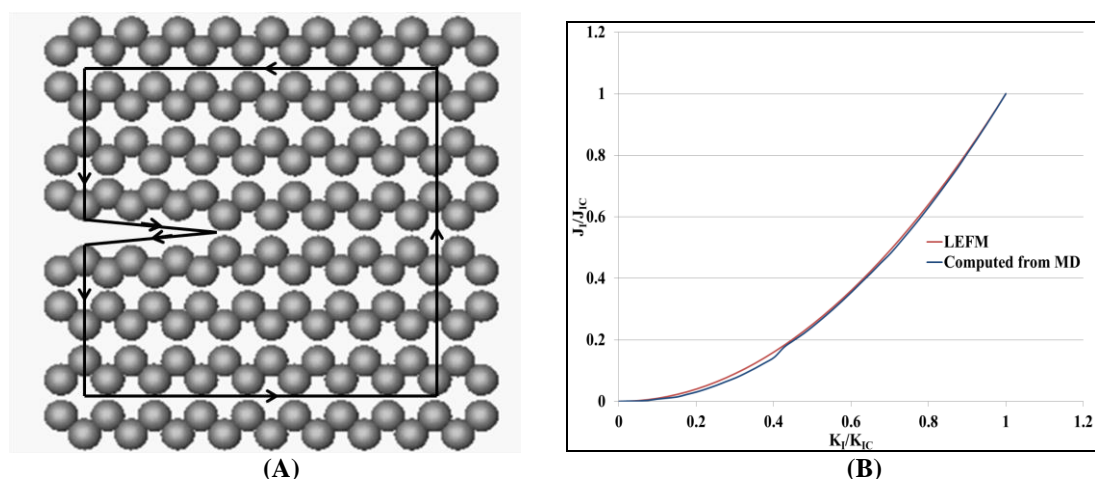


Figure 5. Atomistic J-integral computation in mode-I nanoscale crack propagation in a single graphene platelet. (A) A graphene sheet with nanoscale crack and contour for J-Integral computation; (B) Normalized atomistic J-integral value at $T=0$ K for graphene sheet at different applied stress levels.

6 Discussion

It is envisioned that a better understanding of the strength enhancement mechanisms at the nanoscale will lead to optimization of materials processing variables at the macroscale, which in turn will lead to the manufacture of nanocomposites more efficiently and at lower cost. The proposed multi-scale analysis will help provide insight into the nanoscale interactions that are responsible for toughening/strengthening mechanisms in nanocomposite systems at the macro-scale. The work presented in this paper will help in evaluating properties such as work of separation at nanoscale and incorporate them at higher length scales using multi-scale modeling methods.

7 Acknowledgment

The authors would like to acknowledge sponsorship of this research by NASA Fundamental Aeronautics Research Program (Subsonic Fixed Wing Project), Contract No. NNX11AI32A, with Mr. Brett Bednarczyk as Technical Monitor. The authors would also like to thank Dr. Gregory Odegard and his research group at Michigan Technological University in Houghton, for their assistance with the EPON 862-DETDA polymer modeling using MD.

References

- [1] Roy S., Hussain F., Narasimhan K., Vengadassalam K., and Lu H., E-Glass/Polypropylene Nanocomposites: Manufacture, Characterization, Thermal and Mechanical Properties, *Polymer & Polymer Composites*, **Vol. 15**, No. 2, pp. 91-102, (2007).

- [2] Saether E., Yamakov V. and Glaessgen E., A Statistical Approach for the Concurrent coupling of Molecular Dynamics and Finite Element Methods. *AIAA paper*, Honolulu, HI, AIAA-2007-2169, April (2007).
- [3] Valavala P.K., Clancy T.C., Odegard G.M. and Gates T.S., Nonlinear multiscale modeling of polymer materials. *International Journal of Solids and Structures*, **Vol. 44**, pp. 1161-1179, (2007).
- [4] Buryachenko V.A., Roy A., Lafdi K., Anderson K.L. and Chellapilla S., Multi-scale mechanics of nanocomposites including interface: Experimental and numerical investigation. *Composites Science and Technology*, **Vol. 65**, pp. 2435-2465, (2005).
- [5] Riddick J.C., Frankland S.J.V. and Gates T.S., Multiscale Analysis of Delamination of Carbon Fiber-Epoxy laminates with Carbon Nanotubes. *AIAA paper*, Newport, RI, AIAA-2006-1676, May (2006).
- [6] Awasthi A.P., Lagoudas D.C. and Hammerand D.C., Modeling of Interface Behavior in Carbon Nanotube Composites. *AIAA paper*, Newport, RI, AIAA-2006-1677, May (2006).
- [7] Abraham F.F., Broughton J.Q., Bernstein N. and Kaxiras E., Concurrent coupling of length scales: methodology and application, *Physical Review B*, **Vol. 60**, No. 4, pp. 2391-2403, (1999).
- [8] Ogata S., Lidorikis E., Shimojo F., Nakano A., Vashishta P. and Kalia R.K., Hybrid finite-element/molecular-dynamics/electronic-density-functional approach to materials simulations on parallel computers, *Computer Physics Communications*, **Vol. 138**, pp.143 – 154, (2001).
- [9] Wagner G.J. and Liu W.K., Coupling of atomistic and continuum simulations using a bridging scale decomposition, *Journal of Computational Physics*, **Vol. 190**, pp. 249-274, (2003).
- [10] Ma J., Lu H., Wang B., Hornung R. , Wissink A., and Komanduri R., Multiscale Simulation Using Generalized Interpolation Material Point (GIMP) Method and Molecular Dynamics (MD), *Computer Modeling in Engineering & Sciences*, **Vol. 14**, No. 2, pp. 101-117, (2006).
- [11] Khare R., Mielke S.L., Paci J.T., Zhang S., Schatz G.C. and Belytschko T., Two quantum mechanical/molecular mechanical coupling schemes appropriate for fracture mechanics studies. *AIAA paper*, Honolulu, HI, April (2007).
- [12] Liu W. K., Karpov E. G. and Park H. S., *Nano Mechanics and Materials: Theory, Multiscale Methods and Applications*, J. Wiley & Sons Ltd., U.K, (2006).
- [13] Allen M .P. and Tildesley D. J., *Computer Simulations of Liquids*, Clarendon Press, Oxford, (1987).
- [14] Roy S., Akepati A. R., Hayes N., Multi-scale Modeling of Nano-Particle Reinforced Polymers in the Nonlinear Regime, *Proceedings of the 53rd AIAA-SDM Conference*, Honolulu, HI, April 23-26, (2012).
- [15] Jones R. E., Zimmerman J.A., Oswald J. and Belytschko T., An atomistic J-integral at finite temperature based on Hardy estimates of continuum fields, *Journal of Physics: Condensed Matter*, **Vol. 23**, 1-12, (2011).
- [16] Jones R. E. and Zimmerman J.A., The construction and application of an atomistic J-integral via Hardy estimates of continuum fields, *Journal of Mechanics and Physics of Solids*, **Vol. 58**, 11318-11337, (2010).
- [17] Hardy R., Formulas for determining local properties in molecular dynamics simulations: shock waves, *Journal of Chemical Physics*, **Vol. 76(1)**, 622-628, (1982).